

# Autonomous I-AUV Docking for Fixed-base Manipulation<sup>\*</sup>

Narcís Palomeras<sup>\*</sup> Pere Ridao<sup>\*</sup> David Ribas<sup>\*</sup>  
Guillem Vallicrosa<sup>\*</sup>

*<sup>\*</sup> Computer Vision and Robotics Research Institute  
Scientific and Technological Park of the University of Girona  
CIRS Building C/ Pic de Peguera, CO 17071 Girona  
Catalonia - Spain (e-mail: npalomer@eia.udg.edu).*

---

**Abstract:** While commercially available autonomous underwater vehicles (AUVs) are routinely used in survey missions, a new set of applications exist demanding intervention capabilities. This is the case, for instance, of the maintenance of permanent underwater observatories or submerged oil wells. These tasks, currently undertaken by remotely operated vehicles (ROVs), can be automated using intervention AUVs (I-AUVs) reducing their complexity and costs. The TRITON spanish funded project proposes the use of light I-AUV for autonomous intervention tasks, such as valve turning or connector plugging/unplugging, in adapted sub-sea infrastructures. To this aim, this paper presents the design and implementation of an I-AUV-friendly sub-sea docking panel, as well as the vision-based autonomous docking procedure for the Girona 500 lightweight I-AUV. The panel implements a funnel-based docking method for passive accommodation. It also includes a T valve and a custom designed hot stab connector. Once docked, the I-AUV and the panel become rigid and basic fixed-base manipulation strategies can be used for manipulation.

*Keywords:* Autonomous vehicles, Marine systems, Robot navigation, Robot vision, Robot control, Robotic manipulators.

---

## 1. INTRODUCTION

Different application domains require the capability of undertaking maintenance operations in underwater infrastructures. Oil industry has pioneered this sort of operations commonly using work class remotely operated vehicles (ROVs) to carry out intervention tasks in panels adapted for ROV operations. Common tasks include opening/closing valves, for instance. Similar needs are now present in permanent observatories since they require periodical maintenance operations. In this case, common tasks include downloading huge amounts of data (for isolated, non-tethered observatories), connecting/disconnecting a cable, replacing batteries, instrumentation de-fouling, as well as placing and recovering sensor packages.

Currently, these operations are being done by the oil industry as well as by the oceanographic institutions by means of work class ROVs operated from intervention ships endowed with expensive dynamic positioning (DP) systems and bulky tether management systems (TMS). An step ahead towards increasing the level of autonomy in unmanned intervention systems was demonstrated in the SWIMMER EU project by Evans et al. (2001). In this case an autonomous underwater vehicle (AUV) carrying a

ROV, is launched from a support vessel to autonomously navigate and then to dock into an underwater docking station in an offshore infrastructure. The docking station provides a connection to the AUV and from it to the ROV, allowing a standard ROV operation without the need of a heavy umbilical. The next step towards a fully autonomous intervention system for sub-sea panels was demonstrated with the ALIVE project by Evans et al. (2003). It demonstrated the capability of autonomously docking into a ROV-friendly panel using hydraulic grabs. A very simple automata-based manipulation strategy was used to open/close a valve. The guidance of the vehicle to the panel was done using an imaging sonar when far away and computer vision when nearby. To the best of the authors knowledge this was the first time an autonomous intervention was ever made into a sub-sea panel. In the area of underwater intervention in sub-sea panels, SWIMMER and ALIVE have become milestone projects. Both may represent a cut in the cost thanks to its increased autonomy, which avoids the need for extremely expensive intervention ships with DP and TMS. The aim of the TRITON spanish-funded project is to advance one more step using an extremely light vehicle (i.e. only 200 Kg) in waters up to 500 m. This intervention AUV (I-AUV) is equipped with an electric driven robotic arm to perform multisensory-based manipulation tasks. In this case, the cost will be even reduced because the vehicle will be deployable from very small boats (it is designed to be used with a 7 m boat). Instead of using expensive and bulky hydraulic grabs for docking, this paper proposes the use

---

<sup>\*</sup> This work was supported by the EU funded project PANDORA (Persistent Autonomy through learNing, aDaptation, Observation and ReplAnning") FP7-288273, 2012-2014 funded by the european commission and the Spanish project TRITON DPI2011-27977-C03-02 funded by the ministry of science and innovation.

of a passive accommodation docking system inspired by the one recently presented in the FREESUBNET project by Krupinski et al. (2009). The panel is endowed with a T valve and a custom designed hot stab connector to test different intervention tasks. To the best of the author's knowledge the autonomous plugin/unplugging of a connector has never been demonstrated. A localization filter that merges standard navigation sensors with vision-based updates is proposed to localize the vehicle while a simple cascade control scheme is used to guide the I-AUV during the docking procedure. Extensive results demonstrate the feasibility of the proposed system.

After this introduction, a state of the art in docking systems is given before introducing the funnel-based I-AUV friendly docking station designed in this paper. Sections 4 and 5 describe the I-AUV and the intervention panel localization system as well as the navigation and control scheme. Then, the docking mission at hand is explained and the results obtained with the Girona 500 I-AUV in a water tank are shown before conclusions.

## 2. STATE OF THE ART IN DOCKING SYSTEMS

The docking problem consists in assembling at least two independent rigid bodies to become a single one. In the process, physical and/or logical links are established between both entities. Docking/undocking has an enormous potential for AUV operations. Major reported applications include: launch/recovery, long term deployment, and enhanced underwater intervention systems (see Evans et al. (2001) and Evans et al. (2003)). To achieve these functionalities, different docking station designs have been reported in the literature. Alternatives differentiate among themselves based on: the docking mechanism, its directionality, the homing sensor and the nature of the power/signal link established. In Fukasawa et al. (2003) a landing-based docking (LBD) mechanism is reported. The method, similar to those used to help planes land on aircraft carriers, uses a line tied to the docking station that has to be hooked by a cable deployed from the AUV, forcing it to land over the station that lies on the seabed. With a similar concept, a stinger-based docking (SBD) mechanism was proposed by Lambiotte et al. (2002) for the FAU AUV, with the advantage of allowing four approaching directions for homing instead of a single one. Avoiding the need for (potentially harmful) cables or stingers, a cradle-based docking (CBD) system, approached vertically, and using passive accommodation (0,5 m tolerant) has been the system proposed in the SWIMMER EU project by Evans et al. (2001).

In the context of the Ocean Sampling Networks, an omnidirectional buoy vertical pole (BVP) docking mechanism has been proposed by Singh et al. (2001). The system consist of a vertical pole attached to a bottom assembly and moored to a buoy. The AUV mounts a V-shaped latch at the nose, able to latch the vehicle to the pole. Once latched, a motorized carriage above the AUV descends forcing it to align with the bottom assembly to ensure inductive power and signal connectivity. Funnel docking systems (FDS) consist on a large funnel to help the vehicle accommodation into a tube. In Austin et al. (2006) a FDS is reported being able to detect the presence of the

vehicle and latching it using a clamp, forcing the insertion of a wet mate connector, used for battery charging and data transfer. Grasping-based docking was demonstrated in the ALIVE project by Evans et al. (2003), where an effort was made to allow docking into an unmodified sub-sea panel like those used by the oil industry. In this case, two hydraulic grasps were used to attach the AUV to the handles of a docking panel.

It is clear that the most successful systems demonstrated up to date are the funnel based docking stations. Using them, researchers have reported 90 % reliability in terms of successful docking operations over a series of trials.

An important specification of the docking mechanism is its directionality, while LBD, CBD and FDS are unidirectional systems (homing must be performed in a certain direction), SBD allows 4 homing directions and BVP is omnidirectional. Different navigation sensors have successfully been used for homing in field trials. For instance long baseline (LBL) was used for approaching the sub-sea cradle in SWIMMER, while an orthogonal mechanical scanning sonar was used later to refine the robot position with respect to the cradle prior to docking. Ultra short base line (USBL) is by far the most used sensor (see Austin et al. (2006)) followed by image processing when good visibility conditions hold. In ALIVE, a hybrid approach is proposed where imaging sonar is used to locate and navigate towards the sub-sea intervention panel and computer vision is used for the 3D pose estimation during the final docking process. Besides these more popular approaches, the use of electromagnetic sensors has also been experimented with success for distances below 20 m (see Feezor et al. (2001b)). Finally, it is worth mentioning the methods reported in the literature in order to establish a power/signal link among the AUV and the docking station that include the use of inductive power/signal interfaces by Feezor et al. (2001a), the use of wet mateable connectors by Austin et al. (2006) and the use of radio frequency local access network (RF-LAN) with loop or patch antennas by Lambiotte et al. (2002).

## 3. I-AUV FRIENDLY DOCKING STATION

The design of a mock-up AUV-friendly intervention panel was inspired by the concept described in Krupinski et al. (2009) that are deliverables of the FREESUBNET network. They consist on the installation of funnel-shaped receptacles in the panel and a matching set of probes in the intervention vehicle. Figure 1 shows our current implementation of the concept. As it can be seen, the funnels are installed in the top part of the docking structure and placed in a triangular fashion to match the three probes which are mounted next to each of the vehicle hulls. Given the particular geometry of the Girona 500 I-AUV, this configuration restrains the vehicle displacement, but also the changes in attitude. In our current implementation, the vehicle must exert forward thrust to stay docked. Although we plan to develop a latching system in the future, the current solution has shown capable of maintaining the vehicle in position even in the presence of currents or perturbations due to the intervention task itself.

The flat panel placed in the middle of the funnels is a texture-rich surface which can be easily detected by



Fig. 1. Girona 500 I-AUV with a manipulator attached docked into the mock-up intervention panel.

the vehicle's visual detector system during the docking maneuvers (see Section 4.1). Because of the system's dependance on vision sensors, water turbidity may limit its range of operation. For this reason, in the future, the panel will be equipped with an acoustic transponder for long range guidance to the panel. Two more flat panels are installed on the lower part of the structure. Those contain the mock-ups of a 1/4 turn valve and a hot stab connector, which will be later used to demonstrate the intervention capabilities of the Girona 500 I-AUV.

#### 4. ROBOT AND INTERVENTION PANEL LOCALIZATION

An extended Kalman filter (EKF) is in charge of estimating the vehicle's position ( $[x \ y \ z]$ ) and linear velocity ( $[u \ v \ w]$ ). Vehicle orientation ( $[\phi \ \theta \ \psi]$ ) and angular velocity ( $[p \ q \ r]$ ) are not estimated but directly measured by an attitude and heading reference system (AHRS). This filter is also able to map the pose in the world of several landmarks, thus, working as a simultaneous localization and mapping (SLAM) algorithm. Despite the filter is designed to deal with several landmarks, for the docking task at hand a single one (i.e. the panel) is used. Moreover, instead of localizing the vehicle relative to the panel, we have decided to estimate the absolute position/attitude of both vehicle and panel to simplify the integration of absolute measurements coming from sensors like a global positioning system (GPS) or a USBL. A vision-based system identifies the intervention panel and computes its relative position. This information is introduced in the localization filter as a landmark and is updated with successive observations.

The information to be estimated by the SLAM algorithm is stored in the following state vector:

$$\mathbf{x}_k = [x \ y \ z \ u \ v \ w \ l_1 \ \dots \ l_n]^T \quad (1)$$

where ( $[x \ y \ z \ u \ v \ w]$ ) are vehicle position and linear velocity and ( $l_i = [l_{x_i} \ l_{y_i} \ l_{z_i} \ l_{\phi_i} \ l_{\theta_i} \ l_{\psi_i}]$ ) is the pose of a landmark in world coordinates.

A constant velocity kinematics model is used to determine how the vehicle state will evolve from time  $k-1$  to  $k$ . Landmarks are expected to be static. The predicted state at time  $k$ ,  $\mathbf{x}_k^-$  follows the equations:

$$\mathbf{x}_k^- = f(\mathbf{x}_{k-1}, \mathbf{n}_{k-1}, \mathbf{u}_k, t). \quad (2)$$

$$\mathbf{x}_k^- = \begin{bmatrix} \begin{bmatrix} x_{k-1} \\ y_{k-1} \\ z_{k-1} \end{bmatrix} + \mathbf{R}(\phi_k \theta_k \psi_k) \left( \begin{bmatrix} u_{k-1} \\ v_{k-1} \\ w_{k-1} \end{bmatrix} t + \begin{bmatrix} n_{u_{k-1}} \\ n_{v_{k-1}} \\ n_{w_{k-1}} \end{bmatrix} \frac{t^2}{2} \right) \\ u_{k-1} + n_{u_{k-1}} t \\ v_{k-1} + n_{v_{k-1}} t \\ w_{k-1} + n_{w_{k-1}} t \\ l_{1_{k-1}} \\ \dots \\ l_{n_{k-1}} \end{bmatrix} \quad (3)$$

where  $t$  is the time period,  $\mathbf{u} = [\phi \ \theta \ \psi]$  is the control input determining the current vehicle orientation and  $\mathbf{n} = [n_u \ n_v \ n_w]$  is a vector of zero-mean white Gaussian acceleration noise whose covariance, represented by the system noise matrix  $\mathbf{Q}$ , has been set empirically:

$$\mathbf{Q} = \begin{bmatrix} \sigma_{n_u}^2 & 0 & 0 \\ 0 & \sigma_{n_v}^2 & 0 \\ 0 & 0 & \sigma_{n_w}^2 \end{bmatrix} \quad (4)$$

Associated with the state vector  $\mathbf{x}_k$  there is the covariance matrix  $\mathbf{P}_k$ . Following standard EKF operations, the covariance of the prediction at time  $k$  is obtained as:

$$\mathbf{P}_k^- = \mathbf{A}_k \mathbf{P}_{k-1} \mathbf{A}_k^T + \mathbf{W}_k \mathbf{Q}_{k-1} \mathbf{W}_k^T, \quad (5)$$

where  $\mathbf{A}_k$  is the Jacobian matrix of partial derivatives of  $f$  with respect to the state (1) and  $\mathbf{W}_k$  is the Jacobian matrix of partial derivatives of  $f$  with respect to the process noise  $\mathbf{n}$ .

Three linear measurement updates are applied in the filter: pose, velocity and landmark updates. Each sensor measurement is modeled as:

$$\mathbf{z}_k = \mathbf{H} \mathbf{x}_k + \mathbf{s}_k, \quad (6)$$

where  $\mathbf{z}_k$  is the measurement itself,  $\mathbf{H}$  is the observation matrix that relates the state vector with the sensor measurement, and  $\mathbf{s}_k$  is the sensor noise. Updates are applied by means of the equations:

$$\mathbf{K}_k = \mathbf{P}_k^- \mathbf{H}^T (\mathbf{H} \mathbf{P}_k^- \mathbf{H}^T + \mathbf{R})^{-1}, \quad (7)$$

$$\mathbf{x}_k = \mathbf{x}_k^- + \mathbf{K}_k (\mathbf{z}_k - \mathbf{H} \mathbf{x}_k^-), \quad (8)$$

$$\mathbf{P}_k = (\mathbf{I} - \mathbf{K}_k \mathbf{H}) \mathbf{P}_k^-, \quad (9)$$

where  $\mathbf{K}_k$  is the Kalman gain,  $\mathbf{R}$  the measurement noise covariance matrix and  $\mathbf{I}$  an identity matrix. Below, it is shown how to define  $\mathbf{z}_k$  and  $\mathbf{H}$  for each sensor to perform the updates applying equations (7)-(9).

Several sensors provide position information, which can be used to initialize the vehicle position and bound dead-reckoning errors. A GPS receiver measures vehicle position in the plane ( $x, y$ ) while the vehicle is at the surface, a pressure sensor transforms pressure values into depth ( $z$ ) and a USBL device measures vehicle position ( $x, y, z$ ) while submerged. To integrate any of these position sensors is applied:

$$\mathbf{z}_k = [x \ y \ z] \quad (10)$$

$$\mathbf{H} = [\mathbf{I}_{3 \times 3} \ \mathbf{0}_{3 \times 3} \ \mathbf{0}_{3 \times 6n}] \quad (11)$$

where  $\mathbf{I}_{3 \times 3}$  denotes the  $3 \times 3$  identity matrix and  $\mathbf{0}_{3 \times 6n}$  denotes the  $3 \times 6n$  zero matrix with  $n$  being the number of landmarks. If only ( $x, y$ ) or ( $z$ ) is available,  $\mathbf{z}_k$  and  $\mathbf{H}$  have to be properly arranged.

Velocity updates are provided by a doppler velocity log (DVL) sensor that measures linear velocities with respect to the sea bottom or the water below the vehicle.

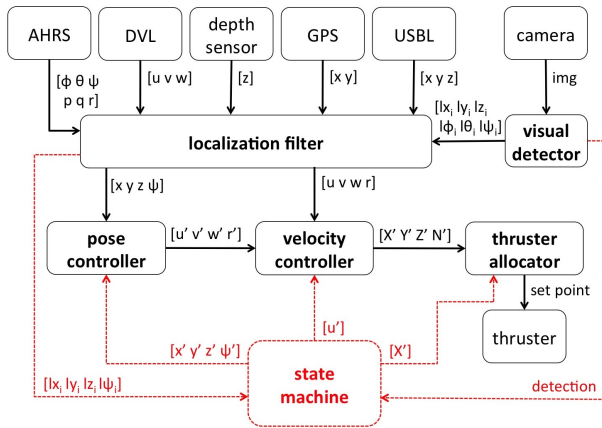


Fig. 2. Schema of nodes that take part in the localization, navigation and control of Girona 500 I-AUV.

$$\mathbf{z}_k = [u \ v \ w] \quad (12)$$

$$\mathbf{H} = [\mathbf{0}_{3 \times 3} \ \mathbf{I}_{3 \times 3} \ \mathbf{0}_{3 \times 6n}] \quad (13)$$

When only velocity updates are available, the filter behaves as a deadreckoning algorithm that drifts over time. However, if position updates or landmarks are detected, the localization filter is able to keep its error bounded.

To identify the inspection panel and compute its pose a vision-based algorithm is used. This algorithm computes the panel relative position as well as its orientation. This information is introduced in the localization filter as a landmark to improve both vehicle and panel position.

$$\mathbf{z}_k = [L_x \ L_y \ L_z \ L_\phi \ L_\theta \ L_\psi] \quad (14)$$

$$\mathbf{H} = \begin{bmatrix} -\mathbf{Rot}^T & \mathbf{0}_{3 \times 3} & \mathbf{Rot}^T & \mathbf{0}_{3 \times 3} & \dots \\ \mathbf{0}_{3 \times 3} & \mathbf{0}_{3 \times 3} & \mathbf{0}_{3 \times 3} & \mathbf{I}_{3 \times 3} & \dots \end{bmatrix} \quad (15)$$

where  $[L_x \ L_y \ L_z]$  is the relative position of the landmark with respect to the vehicle,  $[L_\phi \ L_\theta \ L_\psi]$  is the landmark orientation with respect to the world and  $\mathbf{Rot}$  is the vehicle orientation rotation matrix.

Figure 2 presents a block diagram that shows how each navigation sensor is related with the localization filter. The state vector is initialized according the GPS and pressure sensor or the USBL if it is present and the vehicle is submerged. Linear velocities are set to zero. No landmarks are present when the filter is initialized. The first time that the inspection panel is identified, its pose is introduced in the state vector as a landmark by compounding its relative position, with respect to vehicle's position; being this position the one contained in the state vector.

#### 4.1 Vision-Based docking detector algorithm

To compute the position of a known landmark (i.e. the sub-sea panel) using vision, the images from the camera are compared against an *a priori* known template. Features between the camera image and the template are detected and then matched. It is possible to detect the presence of the landmark, as well as accurately estimate its pose when a sufficient number of features are matched. In this algorithm, the oriented FAST and rotated BRIEF (ORB) feature extractor introduced by Rublee et al. (2011) has been chosen for its suitability to real-time applications.

A minimum number of keypoints must be matched between the template and the camera image to satisfy the

landmark detection requirement. The correspondences between the template and camera image are used to compute the transformation (or homography). Then, using the known geometry of the landmark and the camera matrix, the pose of the landmark in the camera coordinate system and consequently in the vehicle coordinate system can be determined.

## 5. NAVIGATION AND CONTROL

The Girona 500 I-AUV can be actuated in 4 degrees of freedom (DoF) (surge, sway, heave and yaw) while it is stable in roll and pitch. It can be controlled by means of body force requests ( $[X', Y', Z', N']$ ), body velocity requests ( $[u', v', w', r']$ ) and waypoint request ( $[x', y', z', \psi']$ ). A cascade control scheme is used to link these controllers as shown in Fig. 2.

The first controller is a 4 DoF proportional-integral-derivative (PID) called pose controller. It receives as inputs the vehicle pose ( $[x, y, z, \psi]$ ) and the desired waypoint ( $[x', y', z', \psi']$ ). The pose controller output is the desired velocity. The standard PID form is used:

$$v'(t) = K_p \left( e(t) + \frac{1}{T_i} \int_0^t e(\tau) d\tau + T_d \frac{d}{dt} e(t) \right), \quad (16)$$

where  $e(t)$  is the error for each DoF  $[e_x, e_y, e_z, e_\psi]$  computed as

$$\begin{bmatrix} e_x \\ e_y \\ 1 \end{bmatrix} = \begin{pmatrix} \mathbf{R}(\psi)^T & -\mathbf{R}(\psi)^T \\ \mathbf{0}_{1 \times 2} & 1 \end{pmatrix} \begin{bmatrix} x \\ t \end{bmatrix} \begin{bmatrix} x' \\ y' \\ 1 \end{bmatrix},$$

$$e_z = z' - z,$$

$$e_\psi = \text{normalized}(\psi' - \psi), \quad (17)$$

where  $\mathbf{R}$  is a 2D rotation matrix.

The pose controller output ( $\nu'$ ) is sent to the velocity controller together with vehicle's current velocity ( $\nu$ ) following the cascade scheme. The velocity controller computes the desired force and torque by combining a 4 DoF PID (16) with an open loop model-based controller. Here,  $e(t)$  is computed directly by subtracting the desired velocity for each DoF to the current one (e.g.  $e_u = u' - u$ ). The open loop model-based controller generates the force and torque needed to keep a constant velocity without considering the vehicle's current velocity.

$$\tau' = \text{PID}(\nu, \nu') + \text{Model}(\nu'). \quad (18)$$

The output of this controller is the desired force and torque ( $\tau'$ ) defined in the vehicle's body frame. To obtain the force that each thruster has to generate this  $\tau'$  is multiplied by a thruster allocation matrix. Next, a simple thruster model is applied to transform thruster forces into setpoints.

Two motion modes have been implemented to guide the vehicle. The first one follows the whole cascade scheme moving the AUV holonomically by sending waypoint requests to the pose controller. However, if the waypoint to be reached is far from vehicle's current position this motion mode is very slow. Then a variation of line-of-sight (LOS) pure pursuit guidance described in Fossen (2011) is used. The orientation error ( $\psi_e$ ) between vehicle's current pose and the desired waypoint is computed (19) and sent to the pose controller together with the desired depth ( $z'$ ).

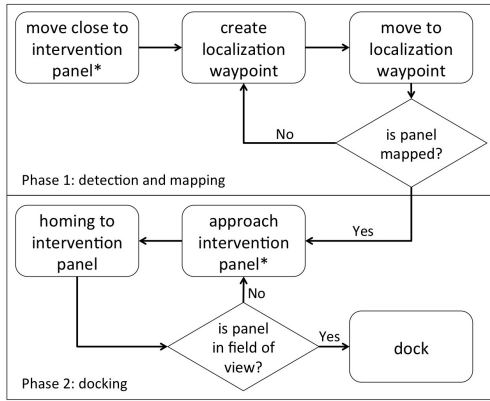


Fig. 3. State machine describing the two phases of the autonomous docking mission. (\*) indicates LOS motion mode.

$$\begin{aligned} \Delta_x &= x'(t) - x(t), \\ \Delta_y &= y'(t) - y(t), \\ \psi_e(t) &= \text{atan2}(\Delta_y, \Delta_x). \end{aligned} \quad (19)$$

When,  $\psi_e(t)$  is smaller than a defined error (*angle\_error*), the desired surge ( $u'$ ) is sent directly to the velocity controller following:

$$\begin{aligned} u'(t) &= \min \left( \frac{\sqrt{\Delta_x^2 + \Delta_y^2}}{\text{approach\_factor}}, 1 \right) \cdot \\ &\left( 1 - \frac{|\psi_e(t)|}{\text{angle\_error}} \right) \cdot \text{max\_surge}, \end{aligned} \quad (20)$$

where *angle\_error*, *approach\_factor* and *max\_surge* are user-defined constants that in our case take the following values: 0.3 rad, 4 and 0.6 m/s respectively. It is worth noting that using this second motion mode, the vehicle's final position contains a larger error than using the first mode and also, the final AUV orientation's ( $\psi$ ) does not correspond to the waypoint's desired orientation ( $\psi'$ ).

## 6. AUTONOMOUS DOCKING TASK

The docking task is split in two phases: first, the I-AUV has to move close to the intervention panel while mapping its pose using the visual detector and the localization filter; and second, the vehicle has to dock into the panel. To have a rough idea about where the panel is, we consider to equip the sub-sea panel with a transponder and using a particle filter estimate its position as has already been done in Becker et al. (2012). However, this preliminary step is out of the scope of this paper and will be developed in future work. Thus, the first step proposed in Fig. 3 is to navigate close to the position estimated by this algorithm using the LOS motion mode. Next, a state machine generates a waypoint around the estimated panel position. While the vehicle moves to this waypoint, the visual detector should be able to identify and map the intervention panel. If this is not possible, a new waypoint is generated and the vehicle is moved to it. If after several waypoints the panel is still undetected, the mission is aborted. Otherwise, when the visual detector identifies and maps the panel, phase two starts. With the panel mapped, the vehicle localization improves significantly due to the visual feedback provided

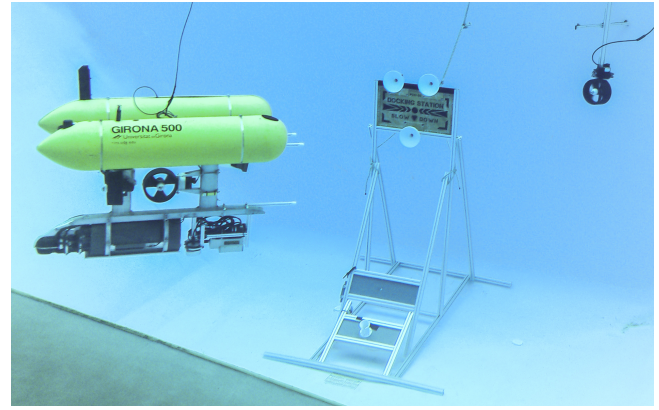


Fig. 4. Experimental setup in the water tank with the Girona 500 I-AUV, the intervention panel, and the thruster to produce perturbations.

by the visual detector every time that the intervention panel is detected. The state machine generates a new waypoint just in front of the mapped panel at a distance in which the intervention panel should be inside the vehicle's field of view. This waypoint may be used later as a recovery position if next step fails. From this position, the vehicle starts the homing procedure to the intervention panel moving holonomically until the probes and the panel funnels are totally aligned and almost touching. If during this process the visual detector is unable to detect the intervention panel, the homing step is aborted and the vehicle returns to the previous defined recovery waypoint. On the other hand, if the panel is detected as expected, a final forward movement is executed by requesting a force in the X-axis through the thruster allocator node while keeping the current depth and yaw angle. This last step produces the passive coupling of both systems. To keep the AUV connected to the intervention panel it is necessary to maintain the forward thrust with a desired force (i.e. 40N) during the intervention operations.

## 7. RESULTS

The results presented in this paper are focused on the second phase of the docking task. A mock-up intervention panel has been mounted in a water tank of  $16 \times 8 \times 5$  m with a Seaeye MCT 1 thruster assembled next to it to simulate water current perturbations during the docking procedure. The Girona 500 I-AUV is equipped with a Teledyne Explorer DVL, a Valeport sound velocity and pressure sensor, a Tritech AHRS, and a Bumblebee2 camera as well as the passive docking system consisting of three probes (see Fig. 4). The AUV was teleoperated around the docking panel until this was identified and mapped by the vision-based detection system. Then, the vehicle was manually moved to a random position in the water tank and the autonomous docking task began.

This procedure was repeated 12 times with only one failure (i.e. successful rate > 90%). In half of these tests random currents in front of the panel were added. These perturbations were generated with a Seaeye MCT1 thruster whose setpoint was changed every 20 seconds and randomly chosen between the 30% and 70% limits of its maximum 14 kg of forward thrust. The generated current was measured

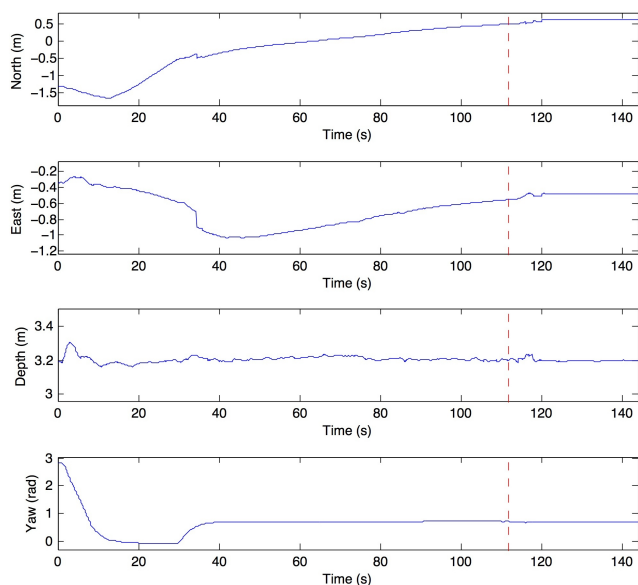


Fig. 5. Resulting trajectory in one experiment.

in vehicle's body as an external force between 3 and 20 Newtons.

Each trial started with the vehicle approaching the intervention panel using the LOS motion mode. The waypoint to reach was computed at 2.0 m from the panel taking into account its orientation. From this position the vehicle faced the docking panel and reached a pose at 70 cm from the panel in which the vehicle probes almost touched the funnels in the panel. Note that all positions are measured from the vehicle's center to the panel's surface. The holonomic motion mode was used to reach this second waypoint. While the vehicle was reaching this waypoint visual updates were present, if they were not, the vehicle should returned to the previous one. This second waypoint was achieved successfully 11 time with a standard deviation of:  $\sigma_{north} = 2.07\text{ cm}$ ,  $\sigma_{east} = 3.76\text{ cm}$ ,  $\sigma_{down} = 1.9\text{ cm}$ , and  $\sigma_{yaw} = 0.76^\circ$ . These errors are small enough to keep the vehicle probes within the entrance of the panel funnels. Therefore, when the last step is executed, and the vehicle pushes forward, the mechanical devices guide the robot until its final position. The average time to complete the docking procedure is 115 seconds. Figure 5 shows one of these tests. It is worth noting that at second 35 there is a significant change in the *North* and *East* axis. This is because the panel was detected after several seconds without detections and vehicle's position was recomputed to agree with the panel's estimated position. The dashed line at second 112 indicates the moment in which the I-AUV reached the final desired waypoint. Few seconds later small perturbations in all the axis shown that the mechanical coupling was achieved.

## 8. CONCLUSION

The design and implementation of an I-AUV-friendly subsea docking panel, as well as the localization and control scheme for the Girona 500 I-AUV have been presented. The panel implements a funnel-based docking method for passive accommodation as well as a T valve and a custom designed hot stab style electric connector. The localization

filter combines standard navigation sensors with visual updates from a vision-based detection algorithm. The docking task has been tested in a water tank demonstrating its high reliability even with external perturbances. As a future work, a transponder will be attached to the intervention panel in order to estimate the panel's pose from far.

## REFERENCES

- Austin, T., Forrester, N., Goldsborough, R., Kukulya, A., Packard, G., Purcell, M., and Stokey, R. (2006). Autonomous Docking Demonstrations with Enhanced REMUS Technology. In *OCEANS 2006 MTS/IEEE*, 1–6.
- Becker, C., Ribas, D., and Ridao, P. (2012). Simultaneous Sonar Beacon Localization & AUV Navigation. In *Proceedings of the 9th IFAC Conference on Manoeuvring and Control of Marine Crafts*. Arenzano, Italy.
- Evans, J., Redmond, P., Plakas, C., Hamilton, K., and Lane, D. (2003). Autonomous docking for Intervention-AUVs using sonar and video-based real-time 3D pose estimation. In *OCEANS, 2003. MTS/IEEE*, volume 4, 2201–2210.
- Evans, J., Keller, K., Smith, J., Marty, P., and Rigaud, O. (2001). Docking techniques and evaluation trials of the SWIMMER AUV: an autonomous deployment AUV for work-class ROVs. In *OCEANS, 2001. MTS/IEEE Conference and Exhibition*, volume 1, 520–528.
- Feezor, M., Yates Sorrell, F., and Blankinship, P. (2001a). An interface system for autonomous undersea vehicles. *Oceanic Engineering, IEEE Journal of*, 26(4), 522–525.
- Feezor, M., Yates Sorrell, F., Blankinship, P., and Bellingham, J. (2001b). Autonomous underwater vehicle homing/docking via electromagnetic guidance. *Oceanic Engineering, IEEE Journal of*, 26(4), 515–521.
- Fossen, T.I. (2011). *Handbook of Marine Craft Hydrodynamics and Motion Control*. John Wiley and Sons.
- Fukasawa, T., Noguchi, T., Kawasaki, T., and Baino, M. (2003). "MARINE BIRD", a new experimental AUV with underwater docking and recharging system. In *OCEANS 2003, MTS/IEEE*, volume 4, 2195–2200.
- Krupinski, S., Maurelli, F., Mallios, A., and Sotiropoulos, P. (2009). Towards AUV docking on sub-sea structures. In *OCEANS 2009 MTS/IEEE*.
- Lambiotte, J., Coulson, R., Smith, S., and An, E. (2002). Results from mechanical docking tests of a Morpheus class AUV with a dock designed for an OEX class AUV. In *OCEANS 2002 MTS/IEEE*, volume 1, 260–265.
- Ruble, E., Rabaud, V., Konolige, K., and Bradski, G. (2011). ORB: An efficient alternative to SIFT or SURF. In *Computer Vision (ICCV), 2011 IEEE International Conference on*, 2564–2571. doi: 10.1109/ICCV.2011.6126544.
- Singh, H., Bellingham, J., Hover, F., Lemer, S., Moran, B., von der Heydt, K., and Yoerger, D. (2001). Docking for an autonomous ocean sampling network. *Oceanic Engineering, IEEE Journal of*, 26(4), 498–514.